AAPS PharmSciTech, Vol. 18, No. 7, October 2017 (© 2017)
DOI: 10.1208/s12249-017-0714-4

Research Article

Clear, Aqueous Topical Drop of Triamcinolone Acetonide

Hoang M. Trinh,[1] Kishore Cholkar,[1,2] Mary Joseph,[1] Xiaoyan Yang,[1] and Ashim K. Mitra[1,3]

Received 18 July 2016; accepted 5 January 2017; published online 9 February 2017

Abstract. The objective of this study was to develop a clear aqueous mixed nanomicellar formulation (NMF) of triamcinolone acetonide (TA) with a combination of nonionic surfactant hydrogenated castor oil 60 (HCO-60) and octoxynol-40 (Oc-40). In order to delineate the effects of drug-polymer interactions on entrapment efficiency (EE), loading efficiency (LE), and critical micellar concentration (CMC), a design of experiment (DOE) was performed to optimize the formulation. In this study, full-factorial design has been used with HCO-60 and OC-40 as independent variables. All formulations were prepared following solvent evaporation and film rehydration method, characterized with size, polydispersity, shape, morphology, EE, LE, and CMC. A specific blend of HCO-60 and Oc-40 at a particular wt% ratio (5:1.5) produced highest drug EE, LE, and smallest CMC (0.0216 wt%). Solubility of TA in NMF improved 20 times relative to normal aqueous solubility. Qualitative ^{1}H NMR studies confirmed the absence of free drug in the outer aqueous NMF medium. Moreover, TA-loaded NMF appeared to be highly stable and well tolerated on human corneal epithelial cells (HCEC) and human retinal pigment epithelial cells (D407 cells). Overall, these studies suggest that TA in NMF is safe and suitable for human topical ocular drop application.

KEY WORDS: aqueous mixed nanomicelles; characterization; critical micellar concentration (CMC); cytotoxicity; experiment design; triamcinolone acetonide.

INTRODUCTION

Diabetic macular edema (DME) is a back-of-the-eye chronic disease caused by the accumulation of fluid in the center of macula which may lead to vision loss (1,2). DME originates from venous occlusions resulting in retina microvascular damage leading to leakage, capillary dropout, upregulation of angiogenic growth factors, and neovascularization (3,4). Diabetes causes degeneration of the inner lining of the blood vessels rendering them porous and leaky. Blood leakage through retinal vasculature causes the center of the retina to swell developing a condition known as DME. Such swelling leads to macular detachment and is responsible for the vision loss. Current treatment of DME includes laser photocoagulation, surgery, intravitreal anti-vascular endothelial growth factor (anti-VEGF), and steroid implant (1, 4–6). Delivery of drugs at therapeutic concentrations to back of the eye tissues (retina/choroid) is a very challenging task. Corticosteroids are prescribed routinely for the treatment of DME. However, steroids have many limitations such as the low aqueous solubility, suboptimal physic-chemical properties, and poor ocular membrane permeability. Steroids are available under implant or intravitreal injection and associate with side effects like inducing intraocular pressure (IOP) leading to glaucoma and cataract (7–9).

TA is a synthetic steroid, possessing anti-inflammatory and anti-angiogenic properties (10). It is highly lipophilic with poor oral bioavailability and systemic side effects. Alternative invasive route of drug administration, i.e., intravitreal injection (IVT) of triamcinolone acetonide (TA), produced promising results for the treatment of DME (11–13). However, IVT is an invasive procedure which is associated with adverse side effects such as retinal detachment, endophthalmitis, pseudoendophthalmitis, intraocular pressure (IOP) elevation, and cataract formation (10, 11, 14). The current delivery strategies for steroids including TA are local administration such as implant and IVT, which are highly invasive and may cause low patient compliance. After IVT administration, TA particles may distribute homogenously in vitreous humor and interfere with vision. Such treatment can also accelerate cataract formation and elevate IOP (15, 16). Therefore, there is an urgent need to develop a clear, aqueous topical eye drop formulation to deliver TA in therapeutic levels to back of the eye tissues (macula region). In such a scenario, aqueous nanomicellar formulation with amphiphilic polymers appears

[1] Division of Pharmaceutical Sciences, School of Pharmacy, University of Missouri–Kansas City, 5258 Health Science Building, 2464 Charlotte Street, Kansas City, Missouri 64108-2718, USA.
[2] RiconPharma LLC, 100 Ford Road, Suite#9, Denville, New Jersey 07834, USA.
[3] To whom correspondence should be addressed. (e-mail: mitraa@umkc.edu)

ABBREVIATIONS μ, micro; mg, milligram'; ppm, parts per million; eq, equivalent; mL, milliliter; FDA, Food and Drug Administration; DME, Diabetic macular edema; TA, Triamcinolone acetonide

to be a promising approach. Hydrophobic TA will be encapsulated in the core of nanomicelles. Hydrophilic corona aids in the development of clear, aqueous solution. This novel nanomicellar strategy may (i) improve drug solubility, (ii) improve drug uptake and cell permeability, (iii) allow for noninvasive delivery of hydrophobic drugs to posterior ocular tissues, and (iv) improve patient acceptability and compliance due to its noninvasive, nonirritating clear, and aqueous system. Nanomicelle structure has been sketched as Fig. 1. Nanomicelles may primarily follow noncorneal pathway such as conjunctival-scleral rather than uveo-sclera pathway after topical administration to reach the retina (17).

In the present study, two amphiphilic polymers, namely hydrogenated castor oil 60 (HCO-60) and octoxynol-40 (Oc-40), are selected. Both HCO-60 and Oc-40 are safe and approved by FDA for human use. Amphiphilic nature of HCO-60 and Oc-40 consist of hydrophobic core and hydrophilic corona allowing spontaneous formation of spherical nanomicelles in aqueous solution. Hydrophobic TA may partition into hydrophobic core of nanomicellar structure whereas the corona is comprised of hydrophilic groups which extend towards surrounding aqueous environment in a manner to stabilize the inner hydrophobic core. The objective of current study is to develop and optimize nanomicellar aqueous TA-loaded formulation utilizing full-factorial statistical design of experiment (DOE). The ratio of the combination HCO-60 and Oc-40 was optimized with JMP 13.0 software and characterized for their size, polydispersity (PDI), shape, surface morphology, EE, LE, and CMC. Standard least square fit analysis was carried out to identify the optimal NMF which generates the highest desirability. Moreover, this formulation was evaluated for *in vitro* cytotoxicity on human corneal epithelial cells (HCEC) and human retinal pigment epithelial cells (D407 cells).

MATERIALS AND METHODS

Materials

TA was obtained from MP Biomedicals, LLC, USA. Hydrogenated castor oil 60 (HCO-60) was procured from Barnet Products Corp., NJ, USA. Octoxynol-40 (Oc-40) (Igepal CA-897) was purchased from Rhodio Inc., NJ, USA. HPLC grade methanol, ethanol, and dichloromethane were purchased from Fisher Scientific, USA. Povidone K 90 (PVP-K-90, Kollidon® 90 F, Ph.Eur, USP) was purchased from Mutchler, Inc. Pharmaceutical ingredients, NJ, USA. CellTiter 96® AQueous nonradioactive cell proliferation assay (MTS) kit and lactate dehydrogenase (LDH) assay kit were obtained from Promega Corp and Takara Bio Inc., respectively. D407 cells were procured from the American Type Culture Collection (ATCC). HCEC are SV-40 virus transfected human immortalized corneal cells; this cell line was a generous gift from Dr. Araki-Sasaki (Kinki Central Hospital, Japan).

Methods

High Performance Liquid Chromatography (HPLC) Analysis

Reversed phase HPLC (RP-HPLC) method was applied to analyze samples with Shimadzu LC pump (Waters Corporation, Milford, MA), Alcott autosampler (model 718 AL), Shimadzu UV/Vis detector (SPD-20AV), and Phenomenex C8 column (Spherisorb 250 × 4.60 mm, 5 μm). The mobile phase was composed of methanol and water (52.5:47.5%*v*/*v*) with the flow rate set at 0.5 mL/min and UV detector at 254 nm. Calibration curve (1 to 25 μg/mL) for TA was constructed by injecting 50 μL into the column.

Experimental Design

Based on the design of experiments (DOE), a preliminary study was conducted to screen the effect of polymers on the formulation variables such as EE, LE, and CMC. In order to develop the experimental design and analyze the data, student version of JMP® 13.0 software (SAS institute, USA) was selected and "Screening design" was adopted. In this study, X1 (HCO-60) and X2 (Oc-40) serve as independent variables. On the other hand, EE (Y1), LE (Y2), and CMC (Y3), respectively, were selected as dependent variables.

Nanomicelle Preparation

Nanomicellar formulations (NMF) were prepared following a previously described procedure reported from our

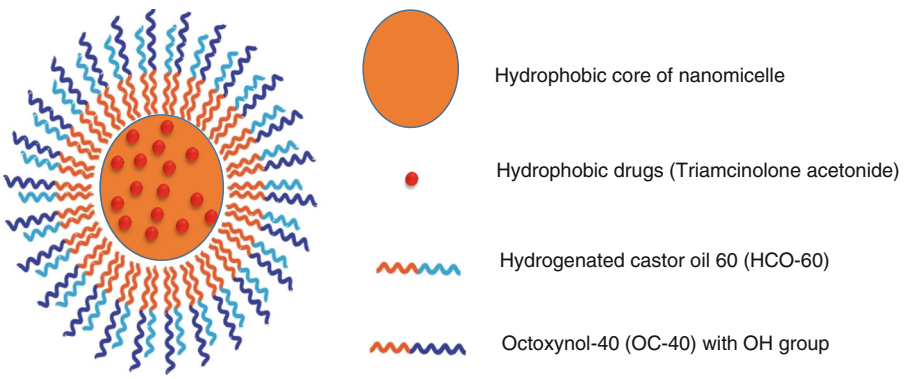

Fig. 1. Schematic drawing image of TA nanomicelle structure

laboratory (17–19). Briefly, HCO-60, Oc-40, and TA were accurately weighed and separately dissolved in ethanol. All three solutions were mixed together to obtain a homogenous solution. Organic solvent was removed under rotary evaporation followed by high vacuum (GeneVac) to generate a thin film. Subsequently, this film was hydrated and resuspended in phosphate buffer. This solution was filtered sterilized through 0.2-μm nylon filter to separate unentrapped TA and other foreign particles. Similarly, the blank formulation was prepared without TA.

Formulation Characterization

Determination of Critical Micellar Concentration (CMC). CMC of single polymer HCO-60, Oc-40, and a binary mixture of HCO-60 and Oc-40 were determined with iodine as hydrophobic probe following a published method from our laboratory (19). The absorbance of hydrophobic iodine partitioned into nanomicellar core was measured with UV–vis spectrometer DDX 880, Beckman Coulter. The absorption intensity was plotted against logarithm of polymer concentration to calculate CMC.

Light Transmittance. The percentage transmittance of light through samples ($N = 4$) was measured at different wavelength range from 400 to 600 nm with a UV–vis spectrometer (Model: Biomate-3, Thermo Spectronic, Waltham, MA). Percent light transmitted was recorded. Distilled deionized water served as blank. All measurements were performed in triplicate.

Viscosity. The viscosity of all the formulations was measured with Ostwald-Cannon-Fenske viscometer following conventional method as previously described (9). Briefly, the travel time or efflux time of NMF and distilled deionized water freely go through ranged distance was measured and calculated with equation 1 (Eq. 1). All measurements were performed in triplicate.

$$\text{Viscosity}_{(\text{liq})} = \frac{\text{Density (liq) X time (liq) X Viscosity(water)}}{\text{Density (water) X time (water)}} \quad (1)$$

where viscosity $_{(\text{water})} = 0.89$ centipoise (Cp), 25°C, and density $_{(\text{water})} = 1$ g/mL

Mixed Nanomicellar Size, Polydispersity Index (PDI), and Surface Potential. The nanomicellar size, PDI, and surface potential were determined by dynamic light scattering analyzer (DLS) (Brookhaven Zeta Plus instrument, Holsville, NY, USA). A sample volume of 500 μL without dilution was subjected to size measurement at a laser wavelength of 659 nm at room temperature. All measurements were performed in triplicate.

Transmission Electron Microscopy (TEM). To determine shapes of TA-loaded NMF, a drop of nanomicelles formulation was placed on TEM grid with carbon film; excess of liquid was removed with filter paper and grid was air dried. Specimens were negatively stained with 1% uranyl acetate and TA nanomicelles were witnessed with CM12 electron microscope (FEI, Hillsboro, OR) at 80 kV accelerating voltage. Image acquisition was performed with Orius CCD camera (GATAN, Pleasanton, CA).

Dilution Study. The dilution effect of NMF was studied by diluting the sample from 0 to 200 times with phosphate buffer. Diluted TA nanomicelles were measured for size characterization following an earlier described protocol (20). Briefly, the TA-loaded NMF were diluted with appropriate volume of phosphate buffer (Table IV) and NMF size and PDI were recorded from DLS analyzer.

Entrapment and Loading Efficiency. Following a published protocol (17), reversed micellization was achieved in organic solvent (dichloromethane) and TA was extracted from the core of nanomicelles. The amount of TA encapsulated within NMF was measured with HPLC. The percentage EE and LE of TA in NMF were calculated with equations 1 and 2.

$$\text{EE}(\%) = \frac{\text{amount of TA quantified in NMF}}{\text{amount of TA added in the NMF}} \times 100 \quad (2)$$

$$\text{LE}(\%) = \frac{\text{amount of TA quantified in NMF}}{(\text{amount of TA added} + \text{amount of polymers used})} \times 100 \quad (3)$$

*1*H NMR Characterization. Proton nuclear magnetic resonance (^{1}H NMR) was applied to identify any unentrapped (or) free TA in the NMF solution. ^{1}H NMR studies were conducted for TA, blank NMF, and TA-loaded NMF. ^{1}H NMR spectra were recorded on Varian 400 MHz spectrometer (Varian, USA) in deuterated water (D_2O) or deuterated chloroform ($CDCl_3$).

Cell Culture. Human corneal epithelial cells (HCEC cells) were cultured following a previously published protocol (18, 21). Briefly, DMEM/F-12 medium comprising of 15% (*v*/*v*) heat inactivated fetal bovine serum (FBS), 22 mM $NaHCO_3$, 15 mM HEPES and 5 mg/L insulin, 10 μg/L human epidermal growth factor, 100 mg/L penicillin, and 100 mg/L streptomycin was prepared. Cells with passage numbers between 15 and 25 were utilized for all studies. Human retinal pigment epithelial cells (D407 cells) were grown as described earlier (17) in DMEM medium supplemented with 10% (*v*/*v*) heat inactivated FBS, 15 mM HEPES, 29 mM $NaHCO_3$, 100 mg/L penicillin, 100 mg/L streptomycin, and 1% nonessential amino acid. Both cell lines were incubated at 37°C, 5% CO_2, and 90% humidity. Both media were changed every alternate day.

Cytotoxicity Assay. In vitro cytotoxicity studies of NMF were carried out with Premix WST-1 cell proliferation assay kit (Takara Bio Inc.) and Lactate dehydrogenase (LDH) assays (Takara Bio Inc.) on HCEC and D407 cells, respectively. Briefly, HCEC and D407 cells were cultured in flasks and harvested at 80–90% confluency with TrypLE™ Express (Invitrogen, Carlsbad, CA, USA). Cells were transferred to 96-well plates at a density of 10,000 cells/well, and cytotoxicity studies were initiated following manufacturing protocol. NMF solution (blank and TA-loaded) were prepared and resuspended in serum-free media and filtered with 0.2 μm nylon membrane to obtain sterile formulations.

Premix WST-1 cell proliferation assay: Experiments were performed following a published method (17). To each well, 100 μL of NMF was added and incubated for 1 h at physiological conditions. Serum-free media and Triton X-100 (10%) served as negative and positive controls, respectively. Following incubation, 10 μL of premixed WST-1 was added to each well, incubated for 30 min, and absorbance was measured for the formazan product at 440 nm. An increase in absorbance of formazan denotes the % viable cells.

LDH assay: To evaluate cell membrane damage caused by NMF in each well, 100 μL of serum-free media and 100 μL NMFs were added and incubated for 1 h at 37°C. Serum-free media and Triton X-100 10% served as negative and positive samples. After incubation period, 96-well plate was centrifuged at 250×*g* for 10 min and 100 μL of supernatant was collected into 96-well flat bottom plate. LDH released from damaged cells was measured with LDH assay kit and absorbance of samples was measured at 490 nm. The % membrane damage was calculated with equation 4 (Eq. 3).

$$\%\ \text{Cytotoxicity} = \frac{\text{exp. value - cell culture medium value}}{\text{Triton X\_100 - cell culture medium value}} \times 100 \quad (4)$$

Drug Release Study. TA release kinetics from NMF was studied following previously described protocol (19). Briefly, TA NMF and TA ethanoic solution (control) were transferred to dialysis bag with a molecular weight cut-off of 1000 Da. The bags were immediately transferred to 15-mL centrifuge tubes, previously thermostated at 37°C, containing 5-mL Dulbecco's Phosphate-Buffered Saline (DPBS) (pH = 7.4) buffer solution. All samples were placed in shaking water bath at 37°C and 60 rpm. At predetermined time points, drug release medium (5 mL) was collected and replaced with equal volume of fresh buffer to maintain sink conditions. Collected DPBS was immediately stored at −80°C until further analysis. Before analysis, samples were thawed, vortexed, and extracted for TA (reverse micellization). Extracted samples were injected into RP-HPLC to determine TA concentrations.

Osmolarity and pH. Osmolarity is an important attribute for the topical eye drop formulation. It was measured using the Wescor Vapor Pressure Osmometer Vapro 5520 follow the manufacture manual. Briefly, 10 μL of NMF was loaded in the center of the sample disc and immediately the instrument measure and show osmolarity value. The pH of the NMF was adjusted similar to the tear pH ~ 6.8 with phosphate buffer.

Statistical Analysis

The experimental design and data analysis were performed by JMP 13.0 software student version. The effect of two factors—polymer (HCO-60 and Oc-40) amounts on dependent variables (EE, LE, and CMC) was studied with statistical models. These models will denote interactive and polynomial influences on the dependent outcome in order to predict fit model (Eq. 4)

$$Y = b_0 + b_1X1 + b_2X2 + b_3X1X2 \quad (5)$$

where Y is response outcome; b_0 denotes intercept; and b_1, b_2, and b_3 represent the regression coefficients for factors X1, X2, and interaction X1 and X2, respectively. X1 denotes amount of HCO-60 and X2 represents amount of Oc-40. The t test at $\alpha = 0.05$ level was used to determine the significant relationship between independent and dependent variables.

In vitro experiments were performed at least in quadruplicate ($n = 4$) and the results were expressed as mean ± standard deviation (SD). Student's t test was applied to compare mean values. And a p value of ≤0.05 is considered as statistically significant.

RESULTS AND DISCUSSION

Experiment Design

In this study, a full-factorial DOE with one center points and one replicate was selected to screen the independent factors for dependent variables. All formulations were characterized for EE, LE, CMC, size, PDI, surface potential, light transmittance, and cytotoxicity. The design runs (coded and uncoded) and corresponding variables are summarized in Table I. The nanomicellar size, PDI, surface potential, and light transmittance did not show significant difference among formulations. The size and distribution of all NMFs were determined by the DLS method and presented in Table II ranging from 20 to 26 nm. The PDI for all run were below 0.45 indication narrow size distribution. All light transmittance were above 90% indicating that the formulations allow the light pass through as close as water. The percent of cell viability of all NMFs were compared with medium and Triton X-100 10% which served as positive and negative controls, respectively (Fig. 2). Because DOE used one replicate, the cytotoxicity only performed from F1 to F5 for both blank NMF and TA-loaded NMF. More than ~80% cell viability was observed as compared to the control, where Triton X-100 generated less than 20% viability. However, a significant

Table I. Design of Experimental (DOE) Coded and Uncoded Runs

Formulation code	Coded design		Uncoded design	
	X1	X2	X1 (HCO-60) (wt%)	X2 (OC-40) (wt%)
F1	+	+	5	3
F2	+	−	5	1
F3	0	0	3.5	2
F4	−	+	2	3
F5	−	−	2	1
F6	+	+	5	3
F7	+	−	5	1
F8	0	0	3.5	2
F9	−	+	2	3
F10	−	−	2	1

Table II. Summary of Uncoded Design and Corresponding EE, LE, CMC, Size, PDI, Zeta Potential, and % Light Transmittance

Formulation code	HCO-60 (wt%)	OC-40 (wt%)	EE (%)	LE (%)	CMC	Size (nm)	PDI	Zeta potential (mV)	T (%)
F1	5	3	55	0.682	0.0380	24.05	0.394	−0.78	98.51
F2	5	1	39	0.645	0.0059	25.04	0.378	−0.469	94.76
F3	3.5	2	35	0.632	0.0385	22.02	0.393	−0.254	93.76
F4	2	3	19	0.379	0.0216	23.08	0.392	+0.418	95.77
F5	2	1	17	0.563	0.0173	25.37	0.404	−0.084	93.05
F6	5	3	57	0.707	0.0380	23.94	0.397	−0.81	98.56
F7	5	1	40	0.662	0.0059	25.13	0.379	−0.458	95
F8	3.5	2	37	0.668	0.0385	22.04	0.393	−0.261	93.76
F9	2	3	20	0.398	0.0216	23.21	0.4	+0.418	95.89
F10	2	1	18	0.596	0.0173	25.07	0.43	−0.089	93.25

HCO-60 hydrogenated castor oil-60, *Oc-40* octoxynol-40, *EE* entrapment efficiency, *LE* loading efficiency, *CMC* critical micellar concentration, *nm* nanometer, *PDI* polydispersity index, *mV* milli Volts, *NMF* nanomicellar formulation, *T* transmittance

difference in EE, LE, and CMC was observed. Therefore, dependent variables such as EE, LE, and CMC were selected to identify the most essential influencing factor for each dependent variable. The standard least square fit analysis in JMP® 13.0 software was conducted, and data was analyzed to identify the most important variables. The parameters and Pareto plot of estimates showed the significant effect with probability for each dependent factor on each outcome. Pareto plots were applied to identify the factors with significant effect on the outcome. The estimated coefficient with $p < 0.05$ was considered to be significant. Results shown in Fig. 3a indicate that different weight percent of HCO-60 and Oc-40 polymers had significant effect ($p < 0.05$) on EE. The Pareto chart shows the significant of HCO-60 ($p < 0.0001$), OC-40 ($p = 0.0003$), and interaction HCO-60*OC-40 ($p = 0.0011$) cumulative percentage effect of the polymer weight percentage (Fig. 3b). The parameter estimates indicate that HCO-60 percentage offer significant contribution on entrapment efficiency relative to Oc-40. The fit model represents the relationship between independent and dependent variables, which are shown in the following equations (Eq. 5):

$$\begin{aligned} Y1 &= 33.7 + 14.625\ X1 + 4.625\ X2 + 3.625\ X1X2\ R^2 \\ &= 0.99,\ p\ \text{value}\ < 0.0001 \end{aligned} \tag{6}$$

where X1(HCO - 60) and X2(Oc - 40).

The correlation coefficient (R^2) for the regression model was 0.99 and a p value less than 0.05 suggests that the model was significant and could predict EE. The model was also validated by plotting the response surface of predictive model for EE as a function of HCO-60 and OC-40 (Fig. 3c).

Similarly, Fig. 4a shows that both HCO-60 and Oc-40 generated significant effect on loading efficiency with probability of 0.0006 and 0.0391, respectively. The regression equation is represented by Eq. 6.

$$\begin{aligned} Y2 &= 0.5922 + 0.09625\ X1 - 0.03875\ X2 + 0.05925\ X1X2 \\ R^2 &= 0.92, p\ \text{value} = 0.0012 \end{aligned} \tag{7}$$

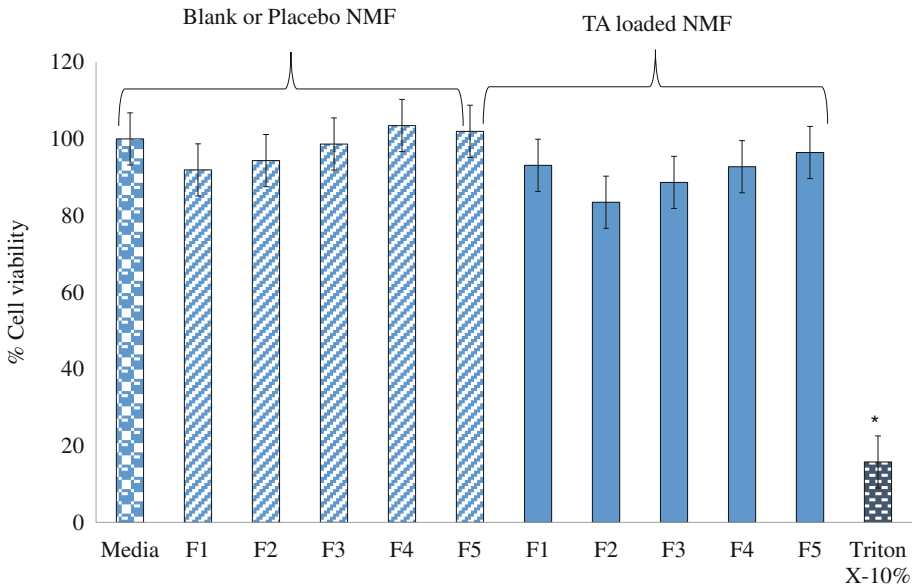

Fig. 2. Cytotoxicity studies conducted on HCEC cells. Cells treated with blank and loaded TA NMFs solutions for 1 h

a

Parameter Estimates

Term	Estimate	Std Error	t Ratio	Prob>|t|
Intercept	33.7	0.558644	60.32	<.0001*
HCO-60(2,5)	14.625	0.624583	23.42	<.0001*
OC-40(1,3)	4.625	0.624583	7.40	0.0003*
HCO-60*OC-40	3.625	0.624583	5.80	0.0011*

b

Sorted Parameter Estimates

Term	Estimate	Std Error	t Ratio	Prob>|t|
HCO-60(2,5)	14.625	0.624583	23.42	<.0001*
OC-40(1,3)	4.625	0.624583	7.40	0.0003*
HCO-60*OC-40	3.625	0.624583	5.80	0.0011*

c

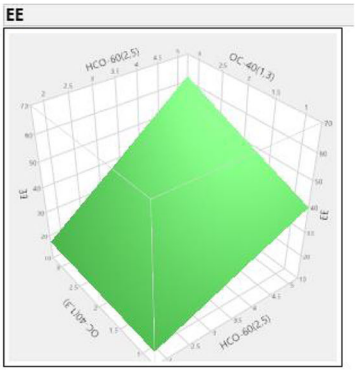

Fig. 3. Summary of variable effects on entrapment efficiency (EE)

The correlation coefficient (R^2) for the regression model was 0.92 and a p value less than 0.05 suggests that the model was significant and could predict LE. The model was also validated by plotting the response surface of predictive model for LE as a function of HCO-60 and OC-40 (Fig. 4b). Since both entrapment and loading efficiency depend on the amount of drug inside the nanomicelle, the prediction models of EE and LE have correlation coefficient very close to each other.

On the other hand, there is no significant effect of HCO-60 polymer observed on CMC (Fig. 5) while OC-40 had lightly effect on CMC with a p value 0.0312. The regression equation is presented by Eq. 7.

$$\begin{aligned} Y3 &= 0.02426 + 0.00125\,X1 + 0.0091\,X2 + 0.00695\,X1X2 \\ R^2 &= 0.68 \quad , \quad p \quad \text{value} \quad = \quad 0.0642 \end{aligned} \tag{8}$$

The correlation coefficient (R^2) for the regression model was 0.68 and a p value greater than 0.05 suggests that the model was not significant.

The prediction profiler was generated to determine the optimal point with highest desirability. It also predicts the combination effects of variables at different levels. Prediction profiler helps to predict the levels of independent variables which may be adjusted to achieve high EE, LE, and low CMC. TA-loaded NMF with such characteristics was assumed to be the better formulation. Prediction profiler indicated that the optimized formula (HCO-60 at 5.0 wt% and OC-40 at 1.5 wt%) may provide optimal EE, LE, and low CMC of 44.0%, 0.676%, and 0.0216, respectively (Fig. 6). This optimized formulation produces the most reasonable desirability between independent and dependent variables. TA-loaded NMF was prepared with HCO-60 and Oc-40 with weight percent predicted by the profiler. EE, LE, and CMC were determined following described earlier procedure and results were summarized in Table III. EE, LE, and CMC for the new NMF were 46%, 0.697%, and 0.0210, respectively. Experimental results appear to be in agreement with the prediction profiler. The DOE was successfully applied to understand the interaction between the polymers and/or drugs and thus achieve the optimal formulation with high desirability. Further, the optimized NMF was subjected to characterization such as size, PDI, surface potential, light transmittance, viscosity, morphology, ^{1}H NMR, dilution effects, cytotoxicity, and *in vitro* release.

Entrapment and Loading Efficiency

TA entrapment and loading into NMFs was determined with RP-HPLC method as described previously. NMFs EE, LE are summarized in Tables II and III. TA is a highly lipophilic drug with poor aqueous solubility 25.4 μg/mL (US

a

Parameter Estimates

Term	Estimate	Std Error	t Ratio	Prob>|t|
Intercept	0.5922	0.01318	44.93	<.0001*
HCO-60(2,5)	0.09625	0.014735	6.53	0.0006*
OC-40(1,3)	-0.03875	0.014735	-2.63	0.0391*
HCO-60*OC-40	0.05925	0.014735	4.02	0.0070*

b

Sorted Parameter Estimates

Term	Estimate	Std Error	t Ratio	Prob>|t|
HCO-60(2,5)	0.09625	0.014735	6.53	0.0006*
HCO-60*OC-40	0.05925	0.014735	4.02	0.0070*
OC-40(1,3)	-0.03875	0.014735	-2.63	0.0391*

c

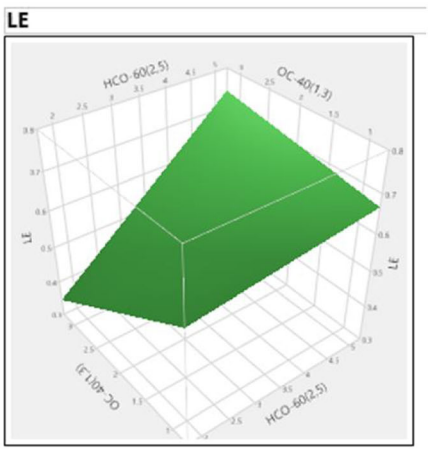

Fig. 4. Summary of variable effects on loading efficiency (LE)

a Parameter Estimates

Term	Estimate	Std Error	t Ratio	Prob>|t|
Intercept	0.02426	0.002907	8.35	0.0002*
HCO-60(2,5)	0.00125	0.00325	0.38	0.7138
OC-40(1,3)	0.0091	0.00325	2.80	0.0312*
HCO-60*OC-40	0.00695	0.00325	2.14	0.0763

b Sorted Parameter Estimates

Term	Estimate	Std Error	t Ratio	Prob>|t|
OC-40(1,3)	0.0091	0.00325	2.80	0.0312*
HCO-60*OC-40	0.00695	0.00325	2.14	0.0763
HCO-60(2,5)	0.00125	0.00325	0.38	0.7138

c

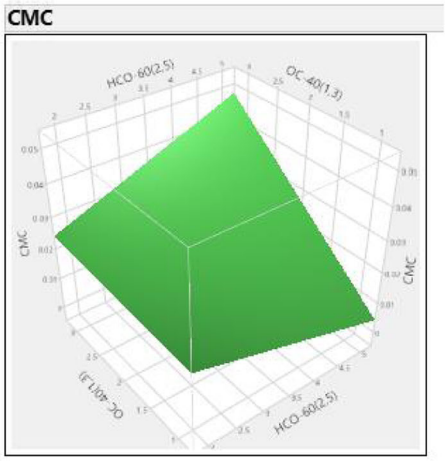

Fig. 5. Summary of variable effects on critical micellar concentration (CMC)

patent US 2006/0141049), and octanol/water partition coefficient is 2.53. Because of the hydrophobic interaction, hydrophobic drug get encapsulated inside hydrophobic core of nanomicelle. Results indicate that entrapment of TA in the core of nanomicelles improved TA solubility by 20 times. Nanomicelle has improved the solubility of TA with increased EE.

Micellar Size, Polydispersity Index (PDI), Surface Charge, or Zeta Potential

Nanomicellar size, polydispersity index (PDI), and zeta potential were determined by dynamic light scattering (DLS). The results are summarized in Tables II and III. Both blank and TA-loaded NMF were in the size range between 20 and 30 nm with narrow distribution. Figure 7a, b illustrated the distribution of blank and TA-loaded NMF. The significantly small size of NMF may sufficiently allow NMF to travel across ocular tissues such as scleral channels/pores, which are in the size range between 20 and 80 nm (22). The PDI of all runs below 0.4 surface charge is negligible. Such property of nanomicelles may help to deliver TA to back of the eyes by the conjunctival/sclera pathway.

Morphology TEM

The morphology of optimal nanomicelle was studied by TEM. Results show that NMFs are spherical in shape with smooth surface architecture without any signs of aggregation (Fig. 8a). Nanomicelles are clearly defined and distinguished as bright, discrete spherical globules on the TEM grid. TA-loaded NMF displays a size of about 20 nm which is in agreement with the size measurement with DLS.

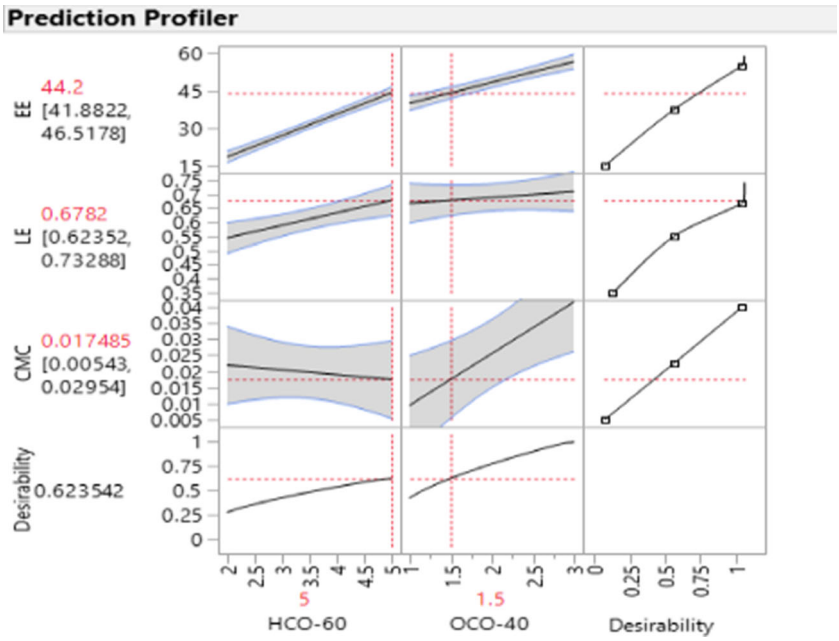

Fig. 6. Prediction profiler for optimized TA NMF

Table III. Characterization of Optimized TA NMF

Formulation code	HCO-60 (wt%)	OC-40 (wt%)	Size (nm)	PDI	Zeta potential (mV)	T (%)	EE (%)	LE (%)	CMC	Viscosity (cP)	Osmolarity (mmol/kg)	pH
Blank optimized NMF	5	1.5	17.01 ± 0.03	0.198	−0.745	96.69	–	–	0.0210	1.897 ± 0.012	300 ± 5.6	6.81
0.1% TA optimized NMF	5	1.5	16.64 ± 0.02	0.200	−0.447	95.58	46 ± 0.6	0.697 ± 0.046	–	1.952 ± 0.014	317 ± 4.5	6.85

Optical Clarity/Appearance

Optical appearance/clarity is defined as the ability of light to be transmitted 90% or more through a 1.0-cm path length at 400-nm wavelength. The major reason for light scattering is due to interference produced by particles. However, particles of extremely small size, i.e., nanometers will not produce enough hindrance or light scattering results in a clear and transparent solution. TA NMF is clear as water (Fig. 8b) or transparent and more than 90% of light has been transmitted (Tables II and III) compared with TA suspension. All NMFs can be compared with distilled deionized water measured by transmittance. Percentage light transmittance of optimized formulations (blank and TA-loaded NMF) at different wavelength range from 400 to 600 nm and from 91 to 96%, respectively (Fig. 9). It was observed that there is no particle interfering with light scattering. The nanomicelles help to develop a clear solution with no solid particles.

Critical Micellar Concentration (CMC)

Ocular static and dynamic barriers are the most challenging barriers for delivery of drugs at therapeutic levels (23). CMC is the most critical factor which regulates drug release in tear film. Only 20% of applied topical drop may be available for absorption (23). Continuous tear production may dilute the NMF which may cause micelle disruption and premature TA release. In order to prevent such disruption, low CMC for nanomicelles are prepared since it imparts high stability to NMF after topical administration. In this study, CMC for blend of HCO-60 and OC-40 was determined and results are summarized in Tables II and III. The optimized formulations display low CMC not accurately in agreement with the prediction profiler. The correlation coefficient (R^2) for the regression model was 0.68 and a p value greater than 0.05 suggests that the model was not significant and not good model in predicting CMC.

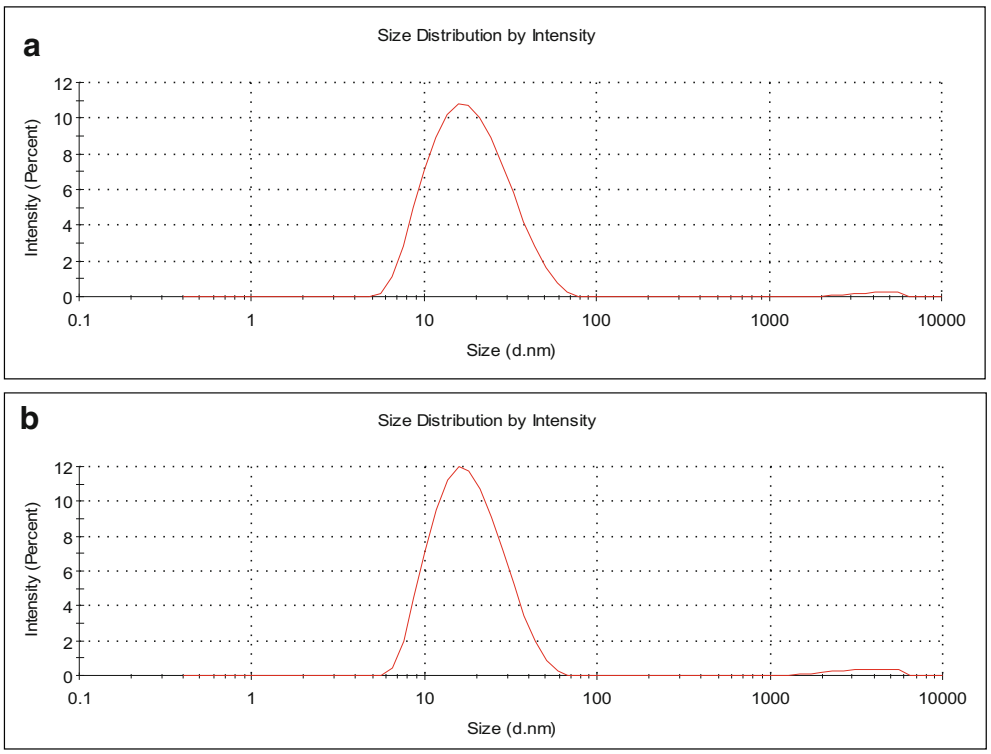

Fig. 7. Size distribution of NMF formulations. **a** Blank NMF. **b** Optimized TA-loaded NMF

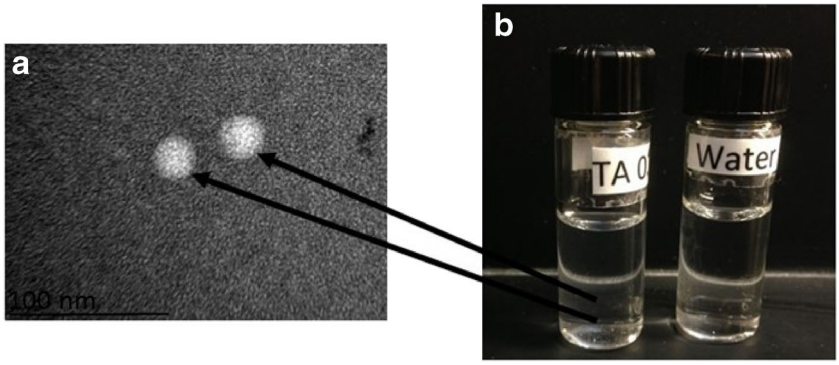

Fig. 8. a Real-time scanning transmission electron microscope (STEM) image of triamcinolone acetonide-loaded nanomicelles (×147,000). *Scale bar* 100 nm. **b** Image showing visual appearance of 0.1% triamcinolone acetonide-loaded nanomicelles on the *left side* in comparison to water on the *right side*

Viscosity

High viscosity of formulation can have effect on its residence time in the cul-de-sac enhancing therapeutic effect. The results summarized in Table III show that NMF produce viscosity less than 2.0 centipoise (cP), well below critical point of 4.4 cP, such that the drainage rate is not affected (24). Formulation viscosity may offer advantages due to longer residence in the cul-de-sac which may increase ocular absorption.

Dilution Effect

Human eyes have many different mechanism and barriers to protect and prevent any harm from external particles from the body. Major ocular barriers are static (corneal epithelium, corneal stroma, and blood–aqueous barrier) and dynamic barriers (blood-retinal barrier, conjunctival blood flow, lymph flow, and tear drainage). Tear drainage is one of those barriers that clear out much of topical application. Therefore, the stability of the NMF was studied upon the effect of dilution. The results in Table IV show that there is no significant effect on nanomicelle size and PDI with dilution up to 200 times.

Osmolarity and pH

Osmolarity is an important attribute for the topical eye drop formulation. The hyper-osmolarity is a main pathogenic factor in dry eye (25). The osmolality and pH of the NMF was adjusted similar to the tear pH ~ 6.8 with phosphate buffer as depicted in Table III. Osmolarity of TA NMF was 317 mmol/kg or mOsm/kg and pH was around 6.8.

^{1}H NMR Characterization

The free drug molecules in solution were identified by ^{1}H NMR analysis at parts per million (ppm) levels. In order to confirm TA entrapment into the mixed nanomicelles core qualitative, ^{1}H NMR spectral analysis was performed in $CDCl_3$ and D_2O. Blank and TA-loaded NMFs were prepared in different solvent such as $CDCl_3$ and D_2O.

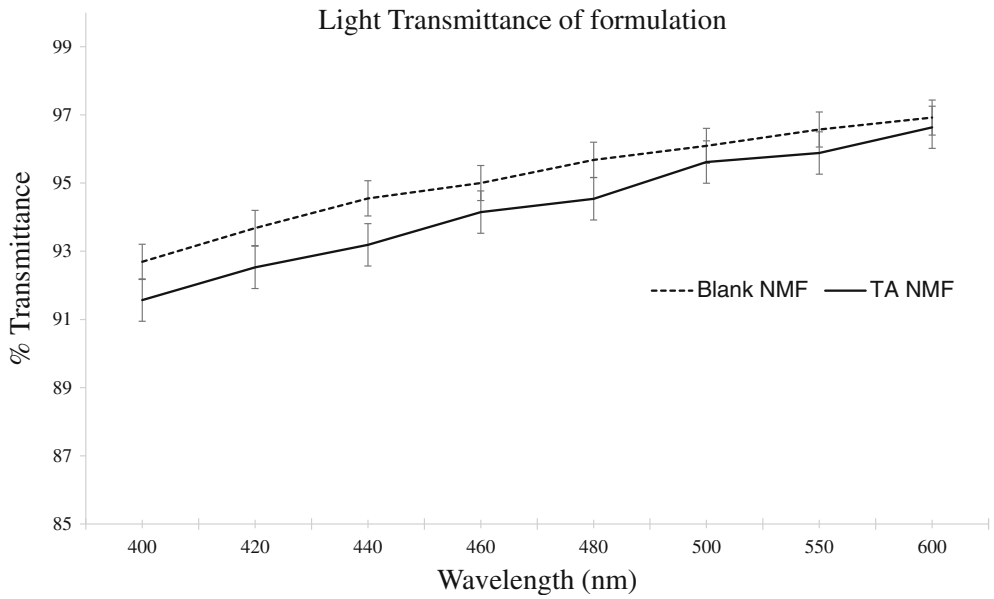

Fig. 9. Light transmittance of formulations (blank, TA NMF)

Table IV. Effect of Dilution on Nanomicellar Size and PDI

Dilution factor	Average size (nm)	PDI
0	16.64	0.200
10	17.02	0.193
20	18.1	0.228
40	17.09	0.233
50	16.86	0.222
100	16.01	0.323
200	18.04	0.360

In Fig. 10a, the resonance peaks were identified with pure triamcinolone acetonide standard in $CDCl_3$. For the blank formulation (Fig. 10b) in chloroform $CDCl_3$, there was no observable peak corresponding to triamcinolone acetonide except polymer peak. However, with the TA-loaded formulation in $CDCl_3$ (Fig. 10d), the resonance peaks similar to pure TA are evident. The spectra indicated that drug is present in organic solvent $CDCl_3$ where reverse micelles are formed. However, resonance signals for TA were absent when suspended in D_2O (Fig. 10c). The results indicate that TA is inside nanomicellar vesicles in aqueous solution. All triamcinolone acetonide in solution was entrapped inside nanomicelles and there was no free/unentrapped TA in the D_2O. Amphiphilic polymers have encapsulated TA inside the core which muted the NMR signal during micelle formulation. This explains the absence of TA signal in D_2O.

In Vitro Cytotoxicity

The formulations/solutions are rapidly washed (within 5 to 10 min) after topical ophthalmic drop instillation into pre-corneal pocket (23). Previous results from our laboratory showed drug molecules in nanomicelles reaching back of the eye tissues (retina/choroid) (26). Therefore, cytotoxicity studies were conducted on human corneal epithelial cells (HCEC cells) and human retinal pigment epithelial cells (D407 cells) for 1-h incubation period. In order to evaluate the cytotoxicity of NMF, WST assay was performed on HCEC. The % cell viability of all NMFs were compared with medium and Triton X-100 10% which served as positive and negative controls, respectively (Fig. 2). Because DOE used one replicate, the cytotoxicity only performed from F1 to F5 for both blank NMF and TA-loaded NMF. More than ~80% cell viability was observed as compared to the control, where Triton X-100 generated less than 20% viability.

In another studies, only optimized formulation was evaluated for cytotoxicity with both WST and LDH (Figs. 11 and 12). The amount of LDH released in the culture medium directly correlates with membrane damage and cytotoxicity. Triton X-100 caused significant toxicity/membrane damage and serves as positive control. LDH study NMF was found to be safe without any cytotoxic effects; the results are compared with the blank culture medium. Results from these assays clearly suggest that NMF do not cause cell death or damage to plasma membrane and are safe and well tolerated for further *in vivo* studies with topical drop application to eye.

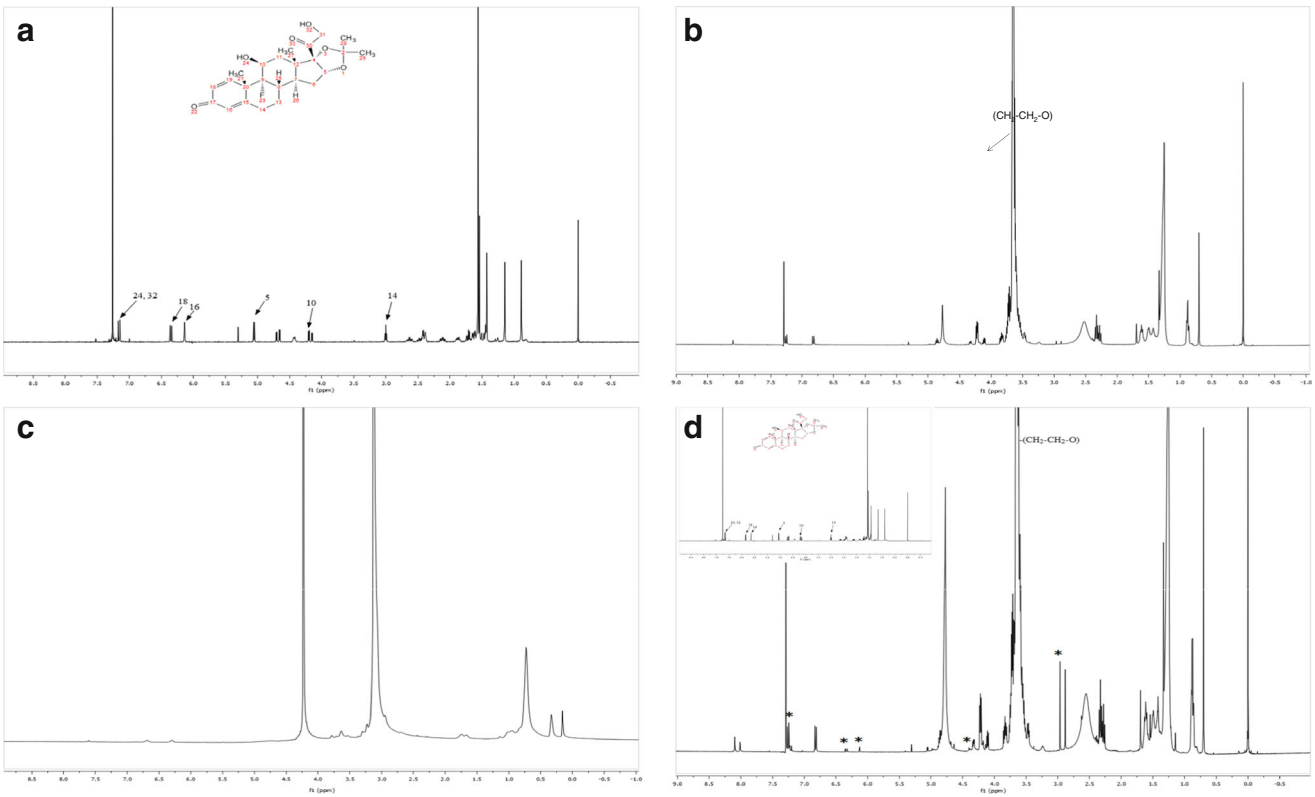

Fig. 10. Qualitative ^1H NMR studies. **a** ^1H NMR spectrum for TA pure drug in $CDCl_3$. **b** ^1H NMR spectrum for placebo polymer micelles in $CDCl_3$. **c** ^1H NMR spectrum for TA nanomicelles in D_2O. **d** ^1H NMR spectrum for TA micelles in $CDCl_3$

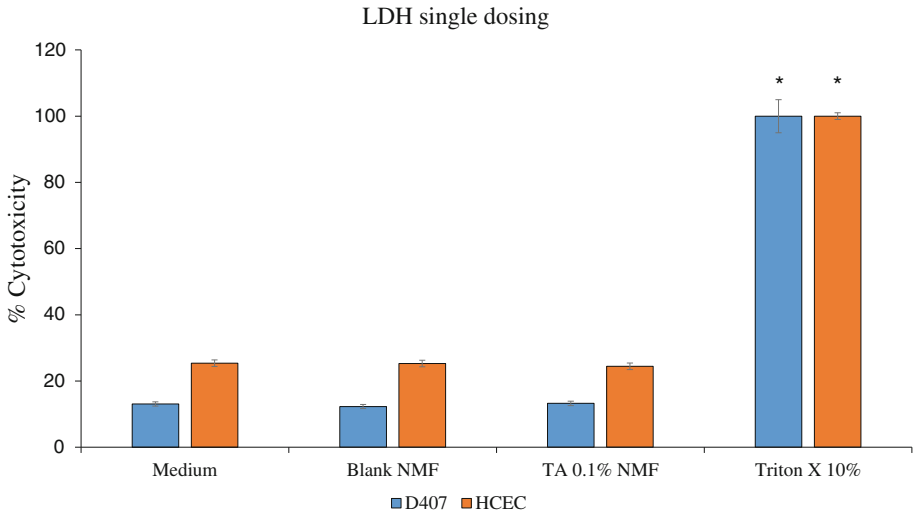

Fig. 11. Cytotoxicity studies (LDH assay) conducted on D407 and HCEC cells. Cells treated with NMF for 1 h

Therefore, these formulations are safe for topical ocular application.

In Vitro Drug Release

To determine the release kinetic of TA from HCO-60 and OC-40 in optimized NMF (F6) was investigated under sink condition at a physiological pH of 7.4 at 37°C. The control represented an equal quantity of TA (1 mg) in 1 mL of absolute ethanol. TA release from NMF was slower than TA release from ethanolic solution. The release kinetic profiles of ethanolic and encapsulated TA from the nanomicelles are illustrated in Fig. 13. Almost 100% of TA was cumulatively released in approximately 24 h from ethanolic TA solution. However, TA release from NMF was very slow (nearly 1 month) without any burst effect. Different drugs have different logP, surface polar area, and the interaction between polymer and drug; the release from nanomicelle will be changed. Results suggest that topical administration of TA NMF helps to sustain release of TA under physiological conditions. Consequently, this nanomicelle formulation may aid in reducing dosing frequency but still achieving therapeutic TA concentrations in ocular tissues.

CONCLUSION

In summary, a clear, stable, aqueous TA-loaded NMF have successfully been optimized and prepared with full-factorial statistical DOE. Results suggest that TA EE was dependent on the combination of polymer HCO-60 and OC-40. Predictive model was produced to determine the amount of independent factors to achieve the highest outcome. The specific blend of HCO-60 at 5.0 wt% and OC-40 at 1.5 wt% generated excellent EE, LE, and low CMC. Optimal TA NMF was clear as water with no light scattering. Nanomicelles are spherical in shape and

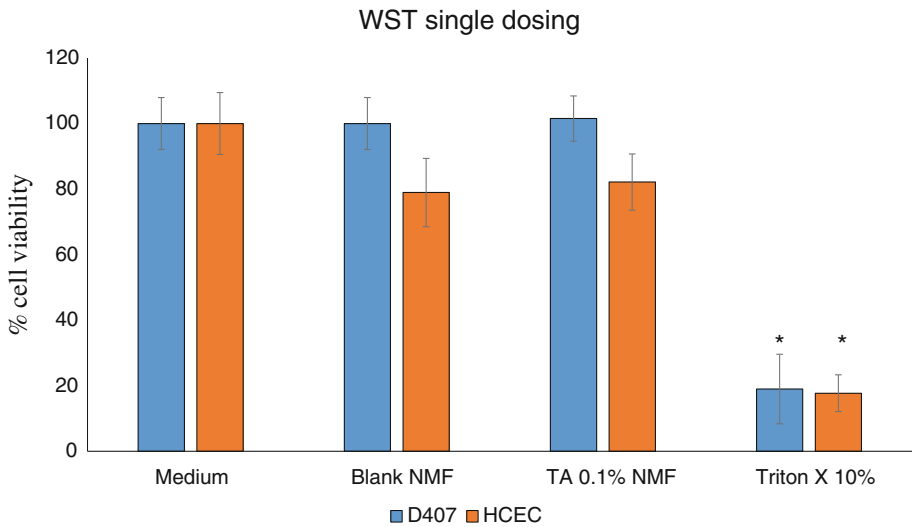

Fig. 12. Cytotoxicity studies (WST assay) conducted on D407 and HCEC cells. Cells treated with NMF for 1 h

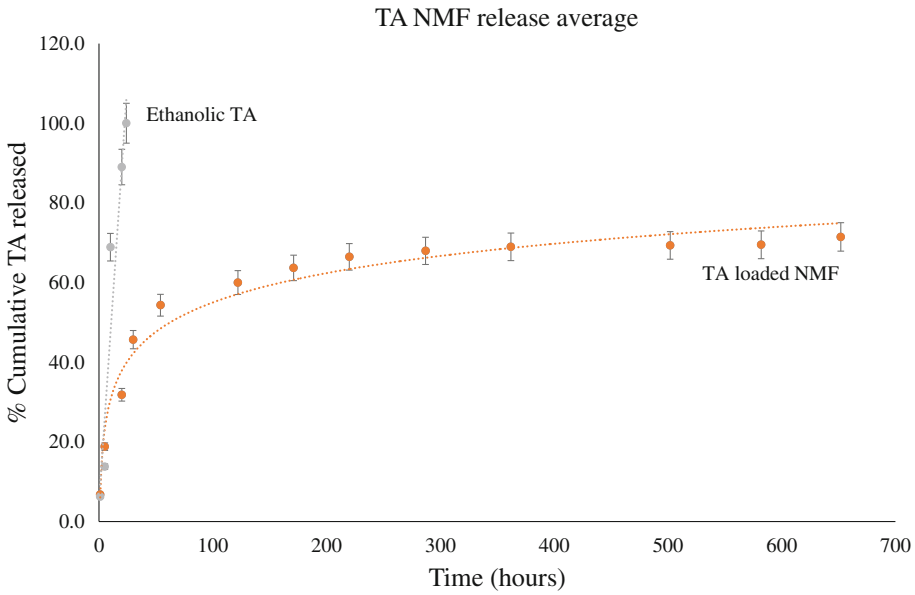

Fig. 13. *In vitro* releases profile of TA from nanomicelles and ethanolic TA solution under sink conditions at 37°C

encapsulated TA in the core NMF display small size, narrow PDI, and are well tolerated in human cell lines. The release profile showed controlled release under physiological conditions. The results indicate that TA NMF may be suitable for human application as ocular drops for anterior and posterior ocular inflammations.

ACKNOWLEDGEMENTS

The authors would like to thank the School of Graduate Studies (SGS), UMKC Research Grant and Graduate Assistant Fund (GAF), and UMKC Women's Council for providing the financial support.

COMPLIANCE WITH ETHICAL STANDARDS

Conflict of Interest The authors declare that they have no conflict of interest.

REFERENCES

1. Trinh, HM, Joseph, M, Cholkar, K, Dhananjay Pal, Mitra, AK. Novel strategies for the treatment of diabetic macular edema. World Journal of Pharmacology. 2016:1–14.
2. Al Rashaed S, Arevalo JF. Combined therapy for diabetic macular edema. Middle East Afr J Ophthalmol. 2013;20(4):315–20.
3. Emerson MV, Lauer AK. Emerging therapies for the treatment of neovascular age-related macular degeneration and diabetic macular edema. BioDrugs : Clin Immunother, Biopharm Gene Ther. 2007;21(4):245–57.
4. Kulkarni AD, Ip MS. Diabetic macular edema: therapeutic options. Diabetes Ther. 2012;3(1):1–14.
5. Jain A, Varshney N, Smith C. The evolving treatment options for diabetic macular edema. Int J Inflamm. 2013;2013:689276.
6. Shamsi HN, Masaud JS, Ghazi NG. Diabetic macular edema: new promising therapies. World J Diabetes. 2013;4(6):324–38.
7. Sihota R, Konkal VL, Dada T, Agarwal HC, Singh R. Prospective, long-term evaluation of steroid-induced glaucoma. Eye. 2008;22(1):26–30.
8. Goni FJ, Stalmans I, Denis P, Nordmann JP, Taylor S, Diestelhorst M, *et al*. Elevated intraocular pressure after intravitreal steroid injection in diabetic macular edema: monitoring and management. Ophthalmol Ther. 2016;5(1):47–61.
9. Friedman DS, Holbrook JT, Ansari H, Alexander J, Burke A, Reed SB, *et al*. Risk of elevated intraocular pressure and glaucoma in patients with uveitis: results of the multicenter uveitis steroid treatment trial. Ophthalmology. 2013;120(8):1571–9.
10. Veritti D, Di Giulio A, Sarao V, Lanzetta P. Drug safety evaluation of intravitreal triamcinolone acetonide. Expert Opin Drug Saf. 2012;11(2):331–40.
11. Smithen LM, Ober MD, Maranan L, Spaide RF. Intravitreal triamcinolone acetonide and intraocular pressure. Am J Ophthalmol. 2004;138(5):740–3.
12. Grover D, Li TJ, Chong CC. Intravitreal steroids for macular edema in diabetes. Cochrane Database Syst Rev. 2008;1, CD005656.
13. Romero-Aroca P. Current status in diabetic macular edema treatments. World J Diabetes. 2013;4(5):165–9.
14. Chu YK, Chung EJ, Kwon OW, Lee JH, Koh HJ. Objective evaluation of cataract progression associated with a high dose intravitreal triamcinolone injection. Eye. 2008;22(7):895–9.
15. Gillies MC, Kuzniarz M, Craig J, Ball M, Luo W, Simpson JM. Intravitreal triamcinolone-induced elevated intraocular pressure is associated with the development of posterior subcapsular cataract. Ophthalmology. 2005;112(1):139–43.
16. Jonas JB, Degenring R, Vossmerbauemer U, Kamppeter B. Frequency of cataract surgery after intravitreal injection of high-dosage triamcinolone acetonide. Eur J Ophthalmol. 2005;15(4):462–4.
17. Cholkar K, Gunda S, Earla R, Pal D, Mitra AK. Nanomicellar topical aqueous drop formulation of rapamycin for back-of-the-eye delivery. AAPS PharmSciTech. 2014.
18. Vadlapudi AD, Cholkar K, Vadlapatla RK, Mitra AK. Aqueous nanomicellar formulation for topical delivery of biotinylated lipid prodrug of acyclovir: formulation development and ocular biocompatibility. J Ocular Pharmacol Ther: Off J Assoc Ocular Pharmacol Ther. 2014;30(1):49–58.
19. Cholkar K, Hariharan S, Gunda S, Mitra AK. Optimization of dexamethasone mixed nanomicellar formulation. AAPS PharmSciTech. 2014;15(6):1454–67.

20. Cholkar K, Gilger BC, Mitra AK. Topical, aqueous, clear cyclosporine formulation design for anterior and posterior ocular delivery. Translat Vision Sci Technol. 2015;4(3):1.
21. Cholkar K, Trinh HM, Vadlapudi AD, Wang Z, Pal D, Mitra AK. Interaction studies of resolvin E1 analog (RX-10045) with efflux transporters. J Ocular Pharmacol Ther: Off J Assoc Ocular Pharmacol Ther. 2015;31(4):248–55.
22. Chopra P, Hao J, Li SK. Iontophoretic transport of charged macromolecules across human sclera. Int J Pharm. 2010;388(1–2):107–13.
23. Cholkar K. Eye: anatomy, physiology and barriers to drug delivery. In: Mitra AK, editor. Ocular transporters and receptors their role in drug delivery: Woodhead publishing; 2013. p. 1–28.
24. Zhu H, Chauhan A. Effect of viscosity on tear drainage and ocular residence time. Optom Vis Sci. 2008;85(8):715–25.
25. Aragona P, Di Stefano G, Ferreri F, Spinella R, Stilo A. Sodium hyaluronate eye drops of different osmolarity for the treatment of dry eye in Sjogren's syndrome patients. Br J Ophthalmol. 2002;86(8):879–84.
26. Meencke HJ. Pathology of childhood epilepsies. Cleve Clin J Med. 1989;56(Suppl Pt 1):S111–20. discussion S21-3.